structures are manifest in different kinetic and thermodynamic parameters for pyr-D-Trp excimer formation in (*R*)-(−)-2-octanol and (*S*)-(+)-2-octanol.

Acknowledgment is made to the donors of the Petroleum Research Fund, administered by the American Chemical Society, for support of this research by a New Directions in Fundamental Research grant.

References and Notes

(1) Horeau, A. *Tetrahedron Lett.* **1969,** 3121.
(2) William, T.; Pitcher, R. G.; Bommer, P.; Gutzwiller, J.; Uskokovic, M. *J. Am. Chem. Soc.* **1969,** *91*, 1871.
(3) Collet, A.; Brienne, M.-J.; Jacques, J. *Bull. Soc. Chim. Fr.* **1972,** 127.
(4) Horeau, A.; Gvette, J. P. *Tetrahedron* **1974,** *30*, 1923.
(5) Kabachnik, M. I.; Mastryvkora, T. A.; Fedin, E. I.; Vaisberg, M. S.; Movozov, L. L.; Petrovsky, P. V.; Shipor, A. E. *Tetrahedron* **1976,** *32*, 1719.
(6) Wynberg, H.; Feringa, B. *Tetrahedron* **1976,** *32*, 2831.
(7) Wynberg, H. *Chimia* **1976,** *30*, 445.
(8) Craig, D. P.; Mellor, D. P. *Fortschr. Chem. Forsch.* **1976,** *63*, 1.
(9) Mason, S. F. *Annu. Rep. Prog. Chem., Sect. A* **1976,** *73*, 53.
(10) Kuroda, R.; Mason, S. F.; Rodger, C. D.; Seal, R. H. *Chem. Phys. Lett.* **1976,** *57*, 1.
(11) Terms chirodiastaltic diastereotropic have been alternatively used to describe the part of interaction between two chiral molecules which discriminate between like and unlike pairs.[8]
(12) (a) Birks, J. B. "Photophysics of Aromatic Molecules"; Interscience: New York, 1973. (b) Birks, J. B., Ed. "Organic Molecular Photophysics"; Interscience: New York, 1973.
(13) Birks, J. B. *Rep. Prog. Phys.* **1975,** *38*, 903.
(14) Craig, D. P.; Power, E. A.; Thrunamachandran, T. *Chem. Phys. Lett.* **1974,** *27*, 149.
(15) Bosnich, B. *J. Am. Chem. Soc.* **1967,** *89*, 6143.
(16) Hayward, L. D.; Totty, R. N. *Can. J. Chem.* **1971,** *49*, 623.
(17) Claesson, S.; Hayward, L. D. *Chem. Phys. Lett.* **1973,** *20*, 85.
(18) Schipper, P. E. *Inorg. Chim. Acta* **1975,** *14*, 161.
(19) Schipper, P. E. *Chem. Phys. Lett.* **1975,** *30*, 323.
(20) Hayward, L. D.; Claesson, S. *Chem. Scr.* **1976,** *9*, 21.
(21) Mason, S. F. *Chem. Phys. Lett.* **1975,** *32*, 201.
(22) Schipper, P. E. *Mol. Phys.* **1975,** *29*, 1705.
(23) Birks, J. B.; Dyson, D. J.; Munro, I. H. *Proc. R. Soc. London, Ser. A* **1963,** *275*, 575.
(24) Birks, J. B.; Christophorou, L. G. *Spectrochim. Acta* **1963,** *19*, 401.
(25) Birks, J. B.; Christophorou, L. G. *Proc. R. Soc. London, Ser. A* **1963,** *274*, 552.
(26) Aladekomo, J. B.; Birks, J. B. *Proc. R. Soc. London, Ser. A* **1964,** *284*, 551.
(27) Noyes, R. M. *Prog. React. Kinet.* **1961,** *1*, 138.
(28) Alwatter, A. M.; Lumb, M. D.; Birks, J. B. In ref 12b, p 403.
(29) Brittain, H. G. *Inorg. Chem.* **1979,** *18*, 1740.
(30) We have also determined parameters for tryptophan to pyrene intramolecular energy transfer in pyr-D-Trp, pyr-L-Trp, and pyr-DL-Trp. Energy-transfer efficiencies of 44.4 ± 0.2 and 45.7 ± 0.2% were obtained for pyr-D-Trp (or pyr-L-Trp) and for pyr-DL-Trp, respectively. Rate constants for the energy transfer, $(1.43 \pm 0.05)10^9$ s^{-1} for pyr-D-Trp (or pyr-L-Trp) and $(2.39 \pm 0.06)10^9$ s^{-1} for pyr-DL-Trp, also showed enantiomeric discriminations. These effects are related to differences in the environments of pyr-Trp. In an optically pure solution of pyr-D-Trp, all the molecules are surrounded by their own kinds. There is a similar situation for pyr-L-Trp. Conversely, in a racemic solution some pyr-D-Trp is surrounded by pyr-L-Trp and some pyr-L-Trp encounters pyr-D-Trp. Since these experiments were carried out at 1.0×10^{-5} M solute concentration, the observed discriminations could not be readily rationalized. Following the referees' comments and the advice of the Editor we have decided to postpone the publication of these and related data until we develop a satisfactory model to rationalize them.
(31) Dwyer, F. P.; Gyarfas, E. C.; O'Dwyer, M. F. *Nature (London)* **1951,** *167*, 1036. Davies, N. R.; Dwyer, F. P. *Trans. Faraday Soc.* **1953,** *49*, 180. Barnes, G. T.; Backhouse, J. R.; Dwyer, F. P.; Gyarfas, E. C. *J. Proc. R. Soc. N.S.W.* **1955,** *89*, 151.
(32) Lianos, P.; Georghiou, S. *Photochem. Photobiol.* **1979,** *29*, 843.

Unified View of Marcus Electron Transfer and Mulliken Charge Transfer Theories in Organometallic Chemistry. Steric Effects in Alkylmetals as Quantitative Probes for Outer-Sphere and Inner-Sphere Mechanisms

S. Fukuzumi, C. L. Wong, and J. K. Kochi*

Contribution from the Department of Chemistry, Indiana University, Bloomington, Indiana 47405. *Received July 11, 1979*

Abstract: Electron transfer rate constants for various homoleptic organometals, especially tetraalkyltin, tetraalkyllead, and dialkylmercury, with tris(1,10-phenanthroline)iron(III), hexachloroiridate(IV), and tetracyanoethylene are compared under standard reaction conditions. Although electron transfer from alkylmetals to FeL_3^{3+} (where L = 1,10-phenanthroline) follows the Marcus correlation with the predicted slope $\alpha = 0.5$ for an outer-sphere mechanism, both $IrCl_6^{2-}$ and TCNE show deviations which vary with the steric hindrance in the alkylmetal, RM. Inner-sphere mechanisms for the latter are also indicated by electron-transfer rates which can be 10^{7-9} times faster than those predicted by the Marcus equation using measured values of the reduction potentials and the reorganizational energies of $IrCl_6^{2-}$ and TCNE. This conclusion is supported by differences in the cleavage selectivities S(Et/Me) for a series of methylethyltin compounds as well as the activation parameters for electron transfer. The Mulliken theory of charge transfer (CT) in TCNE complexes is used to evaluate steric effects in various alkylmetals. The difference ΔE in the charge transfer transition energy $h\nu_{CT}$ of the CT complex relative to that of a reference alkylmetal is assigned to steric effects on the interaction energy associated with ion-pair formation in the successor complex for the inner-sphere mechanism. The result is the linear free energy relationship, $\Delta G^{\ddagger} = \Delta G^{\circ} + \Delta E$, which can be applied to the kinetics of electron transfer from alkylmetals in the absence of steric effects. The unification of Marcus electron transfer and Mulliken charge transfer theories in this manner allows outer-sphere and inner-sphere mechanisms of electron transfer to evolve from a single viewpoint.

Introduction

Historically, the theories of electron transfer in chemical reactions have been developed largely from two quite separate and independent approaches. On one hand, the evolution from inorganic chemistry of oxidation–reduction mechanisms pertaining to transition-metal complexes has led to the Marcus theory, as well as the intervalence transfer theory of Hush.[1,2] The other approach, tracing back to the charge-transfer theory of Mulliken, stems from organic substrates and deals mainly with electronic transitions.[3] Mulliken's theory employs the intermolecular distance between donor and acceptor as the only

0002-7863/80/1502-2928$01.00/0

nuclear parameter, and does not explicitly mention the changes in molecular structure attendant upon charge transfer. On the other hand, the Marcus approach does not readily lend itself to the inclusion of the Franck–Condon factors for the donor and the acceptor. To cover the span of molecular interactions, a unified theory has been presented which reduces to Mulliken's theory in the limit of strong electronic effects (UV and visible regions) and to Hush's theory in the limit of dominating vibrational effects (IR and far-IR regions).[4]

Experimentally, these two theoretical treatments have heretofore remained separate—the Marcus–Hush theory for inorganic redox and electrochemical systems and the Mulliken theory for organic acceptors—because they have lacked a common basis for comparative examination. We believe that organometallic compounds, both as reducing agents and as electron donors, provide such a common basis for comparing electron-transfer and charge-transfer interactions within a framework of steric effects.

The organometals we have chosen are the tetraalkylmetal derivatives R_4M of the group 4 elements, M = lead, tin, germanium, and silicon, as well as the dialkylmercury compounds R_2Hg. These peralkylmetals have tetrahedral (quasi-spherical) and linear (open) configurations, i.e.

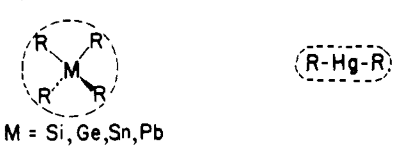

where R represents α- and β-methyl branched alkyl ligands with different steric (E_s) and polar (E_p) properties, as listed in Table I.[5,6] (Consequently, the ionization potentials of these alkylmetals decrease as their steric bulk increases, this opposing trend being more pronounced in the α series than in the β series.) As representatives of organometals generally, these peralkylmetals are particularly useful since they are substitution inert and well behaved in solution for kinetic studies. More importantly, by the proper choice of alkyl ligands in Table I, the ionization potentials and the steric properties of these alkylmetals can be systematically varied and finely tuned to cover wide ranges of subtle molecular effects.

Electron transfer from these alkylmetals can be studied with several diverse types of rather unique reagents, viz., (1) tris(1,10-phenanthroline)iron(III), (2) hexachloroiridate(IV), and (3) tetracyanoethylene. The inorganic oxidants, tris(1,10-phenanthroline)iron(III) (FeL_3^{3+}) and hexachloroiridate(IV), are known to react by outer-sphere mechanisms in a variety of electron-transfer processes, especially with inorganic substrates.[7-9] Likewise, tetracyanoethylene (TCNE) has been widely employed as an electron acceptor in charge transfer spectral studies, particularly with organic π donors.[10] All three reagents, whether they be oxidants or electron acceptors,[11] share a common process with alkylmetals leading to electron transfer. In this report we wish to describe how each can contribute to the delineation of a mechanistic pathway for electron transfer by utilizing *steric effects* as probes to differentiate and to compare the nature of the activation process. In order to establish a basis for doing so, we first summarize the reaction mechanisms by which FeL_3^{3+}, $IrCl_6^{2-}$, and TCNE are known to effect electron transfer from alkylmetals. Schemes I,[12] II,[13-15] and III[16,17] have been separately established by extensive studies of the products and stoichiometry, the energetics and kinetics of the oxidative cleavages, as well as the direct observation or trapping of the paramagnetic intermediates.

Iron(III) complexes FeL_3^{3+}, where L = 2,2′-bipyridine and various substituted 1,10-phenanthrolines, cleave a variety of organometals such as tetraalkyltin according to the general reaction mechanism in Scheme I.[12] The activation process for oxidative cleavage is represented by the electron-transfer step in eq 1. The alkylmetal radical cation is an intermediate, which subsequently undergoes rapid fragmentation in eq 2 rendering the electron transfer irreversible.

Table I. Steric and Polar Parameters for Alkyl Ligands[a]

α-branching			β-branching		
alkyl	E_s	E_p	alkyl	E_s	E_p
methyl	0	0	ethyl	−0.07	0.49
ethyl	−0.07	0.49	*n*-propyl	−0.36	0.55
isopropyl	−0.47	0.85	isobutyl	−0.93	0.58
tert-butyl	−1.54	1.02	neopentyl	−1.74	0.66

[a] In arbitrary energy units from ref 5 and 6.

Scheme I

$$SnR_4 + FeL_3^{3+} \xrightarrow{k_{Fe}} SnR_4^{+\cdot} + FeL_3^{2+} \qquad (1)$$

$$SnR_4^{+\cdot} \xrightarrow{\text{fast}} SnR_3^{+} + R\cdot, \text{ etc.} \qquad (2)$$

For a particular alkylmetal, the rate constant (log k_{Fe}) for electron transfer in eq 1 varies linearly with the standard reduction potential $E°$ of a series of iron(III) complexes with a slope predicted by the Marcus theory for an outer-sphere mechanism, i.e.

$$\log k_{Fe} = 8.5E° + \text{constant} \qquad (3)$$

Moreover, for a particular iron(III) complex, the rate constant (log k_{Fe}) for electron transfer is linearly correlated with the ionization potential I_D of various alkylmetals, i.e.

$$\log k_{Fe} = -4.9I_D + \text{constant} \qquad (4)$$

This remarkable correlation spans a range of almost 10^9 in the rate of electron transfer. Furthermore, the fact that it even includes such hindered alkylmetals as tetraneopentyltin and di-*tert*-butyldimethyltin also indicates that steric effects in the alkylmetal play no significant role in these outer-sphere processes.

Hexachloroiridate(IV) cleaves these alkylmetals by essentially the same reaction mechanism as that described above for the iron(III) complexes, i.e.[13,14]

Scheme II

$$SnR_4 + IrCl_6^{2-} \xrightarrow{k_{Ir}} SnR_4^{+\cdot} + IrCl_6^{3-} \qquad (5)$$

$$SnR_4^{+\cdot} \xrightarrow{\text{fast}} SnR_3^{+} + R\cdot, \text{ etc.} \qquad (2)$$

The activation process for electron transfer to hexachloroiridate(IV) in eq 5, however, differs in two significant ways from that observed with FeL_3^{3+} in eq 1. First, the rate constants k_{Ir} for electron transfer to hexachloroiridate(IV) cannot be derived from the Marcus correlation for iron(III) complexes. Using eq 3 with the reduction potential $E°_{IrCl_6^{2-/3-}} = 0.67$ V and the reorganization energy $\lambda_{IrCl_6^{2-}} = 26$ kcal mol^{-1}, the calculated value of k_{Ir} varies from the experimental one according to the steric properties of the alkyl ligands. Second, the smooth correlation in eq 4 between k_{Fe} and I_D of alkylmetals for outer-sphere electron transfer with iron(III) complexes is no longer valid. Instead, the correlation of the rate constants (log k_{Ir}) for electron transfer to hexachloroiridate(IV) shows considerable but accountable scatter, the magnitude depending on the steric properties of the alkyl ligands. One can conclude from such steric constraints that there is an inner-sphere contribution to electron transfer in the case of hexachloroiridate(IV).

Tetracyanoethylene (TCNE) exhibits transient charge-transfer bands in the electronic spectrum when exposed to the

Table II. Second-Order Rate Constants for Electron Transfer from Tetraalkyltin to Tris(1,10-phenanthroline)iron(III), Hexachloroiridate(IV), and Tetracyanoethylene[a]

no.	R_4Sn	I_D, eV	k_{Fe}	k_{Ir}	k_{TCNE}
1	Me_4Sn	9.69	1.5×10^{-3}	5.2×10^{-5}	1.5×10^{-5}
2	Et_4Sn	8.90	1.3×10	6.3×10^{-4}	8.6×10^{-4}
3	*n*-Pr_4Sn	8.82	4.6×10	4.6×10^{-4}	2.6×10^{-3}
4	*n*-Bu_4Sn	8.76	3.6×10	3.2×10^{-3}	9.1×10^{-3}
5	$EtSnMe_3$	9.10	1.6	1.4×10^{-4}	9.2×10^{-5}
6	*n*-$PrSnMe_3$	9.10	7.9×10^{-1}	5.3×10^{-5}	2.0×10^{-5}
7	*n*-$BuSnMe_3$	9.10	8.5×10^{-1}	3.0×10^{-5}	2.9×10^{-5}
8	Et_2SnMe_2	9.01	5.7	6.9×10^{-4}	4.6×10^{-4}
9	*n*-Pr_2SnMe_2	8.8	1.7×10	1.3×10^{-3}	4.3×10^{-4}
10	*n*-Bu_2SnMe_2	8.8	1.9×10	3.6×10^{-4}	6.3×10^{-4}
11	*i*-Pr_4Sn	8.46	6.9×10^{3}	9.9×10^{-4}	1.4×10^{-3}
12	*sec*-Bu_4Sn	8.45	4.5×10^{3}	5.9×10^{-4}	6.1×10^{-3}
13	*i*-Bu_4Sn	8.68	2.6×10^{2}	1.4×10^{-4}	2.2×10^{-4}
14	*i*-$PrSnMe_3$	8.9		6.5×10^{-3}	6.5×10^{-4}
15	*t*-$BuSnMe_3$	8.6	7.6×10^{2}	7.8×10^{-2}	6.6×10^{-3}
16	*i*-Pr_2SnMe_2	8.56	2.3×10^{3}	6.4×10^{-3}	1.2×10^{-3}
17	*t*-Bu_2SnMe_2	8.22	7.8×10^{4}	9.4×10^{-4}	3.7×10^{-4}
18	*neo*-$Pent_4Sn$	8.67	3.5×10^{2}	$\sim 10^{-6}$	$<10^{-6}$

[a] In acetonitrile solutions at 25 °C. Second-order rate constants in $M^{-1}\,s^{-1}$.

same alkylmetals. It has been shown that the insertion reaction accompanying the disappearance of the charge-transfer complexes proceeds by a rate-limiting electron transfer process in eq 7,[16,17] e.g.

Scheme III

$$SnR_4 + TCNE \overset{K_{CT}}{\rightleftharpoons} [SnR_4\ TCNE] \tag{6}$$

$$[SnR_4\ TCNE] \xrightarrow{k_{CT}} [SnR_4^{+}\cdot TCNE^{-}\cdot] \tag{7}$$

$$[SnR_4^{+}\cdot TCNE^{-}\cdot] \xrightarrow{\text{fast}} [SnR_3^{+}R\cdot TCNE^{-}\cdot], \text{ etc.} \tag{8}$$

Steric effects are manifested in this charge-transfer process in two principal ways. First, it is explicit in the energy $h\nu_{CT}$ of the charge-transfer transition, which according to Mulliken is given by eq 9 developed from second-order perturbation theory for weak complexes:[18]

$$h\nu_{CT} = I_D - E_A - \frac{e^2}{r_{DA}} + \frac{\beta_0{}^2 + \beta_1{}^2}{I_D - E_A - e^2/r_{DA}} \tag{9}$$

where I_D is the ionization potential of the alkylmetal, E_A is the electron affinity of TCNE, and the electrostatic term includes r_{DA}, which is related to the mean intermolecular separation in the CT complex. (The last term in eq 9, including the interaction integrals β_0 and β_1, represents the resonance stabilization due to charge transfer and is roughly equal to the enthalpy of formation, $-2\Delta H_{CT}$.) According to eq 9, if r_{DA} remains unchanged for a series of similar alkylmetals interacting with a common acceptor such as TCNE, ν_{CT} should be linearly related to I_D.[19] Second, in the absence of steric effects the rate constant (log k_{CT}) for electron transfer in eq 7 should correlate with the ionization potential of the alkylmetal, in a manner similar to that observed in eq 4 for iron(III) complexes. Indeed, only a limited correlation of eq 9 is actually observed in the TCNE insertion with the dialkylmercury and methylethyllead compounds. The more extensive series of tetraalkyltin compounds deviate from this correlation in measure with their steric properties, strongly reminiscent of their behavior toward hexachloroiridate(IV), as described above.

In this study, we wish to show how the absence of steric effects in alkylmetals during electron transfer with iron(III) in Scheme I can provide a theoretical basis for evaluating the inner-sphere mechanism with hexachloroiridate(IV) and tetracyanoethylene in eq 5 and 7, respectively. We also wish to establish a more direct and quantitative relationship between electron transfer to hexachloroiridate(IV) as an inner-sphere oxidant and tetracyanoethylene as a charge-transfer acceptor.

Results and Discussion

I. Steric Effects in Electron Transfer from Alkylmetals. Comparison of Phenanthrolineiron(III), Hexachloroiridate(IV), and Tetracyanoethylene. Three series of symmetrical and unsymmetrical tetraalkyltin compounds were the principal focus of this study, viz., R_4Sn, R_2SnMe_2, and $RSnMe_3$, where R = alkyl groups with α- and β-methyl branches. In order to compare electron transfers to $FeL_3{}^{3+}$, $IrCl_6{}^{2-}$, and TCNE, the steric effects in (1) the rate constants k_{Fe}, k_{Ir}, and k_{TCNE} for electron transfer, (2) the selectivities in the cleavage of methylethyltin compounds, and (3) the enthalpy and entropy of activation were measured, as described separately in the following sections. The reactions were all carried out under the same conditions of solvent (acetonitrile) and temperature, as described in more detail in the Experimental Section.

A. Correlation of Electron Transfer Rate Constants. The second-order rate constants k_{Fe}, k_{Ir}, and k_{TCNE} for electron transfer from symmetrical and unsymmetrical tetraalkyltin to $FeL_3{}^{3+}$, $IrCl_6{}^{2-}$, and TCNE, respectively, are listed in Table II. The logarithms of these rate constants are plotted in Figure 1 against the ionization potentials I_D of the tetraalkyltin compounds. It is apparent that only the plot for $FeL_3{}^{3+}$ is linear, those for both $IrCl_6{}^{2-}$ and TCNE showing considerable scatter from any linear correlation. However, despite the random appearance of the plots for both $IrCl_6{}^{2-}$ and TCNE, a closer scrutiny of the data indicates a systematic trend among the sterically hindered alkyltin (compare Tables I and II). These show the most pronounced deviation from the slope of the outer-sphere correlation defined by the points for $FeL_3{}^{3+}$.

B. Selectivity Studies in the Oxidative Cleavage of Methylethyltin Compounds. The cleavage of alkyl ligands from symmetrical tetraalkyltin compounds according to Schemes I–III actually occurs subsequent to the rate-limiting electron transfer. If the same cation is formed as a common intermediate, it should fragment in exactly the same manner in all three processes. The selectivity *S*(Et/Me) for the series of unsymmetrical methylethyltin compounds represents the ratio of first-order rate constants k_{Et}/k_{Me} for the intramolecular competition in eq 10 and 11, where R = Me, Et.[13,16] Selectivity is obtained directly from the analysis of the cleavage products as described in the Experimental Section and compared in Table III for $FeL_3{}^{3+}$, $IrCl_6{}^{2-}$, and TCNE.

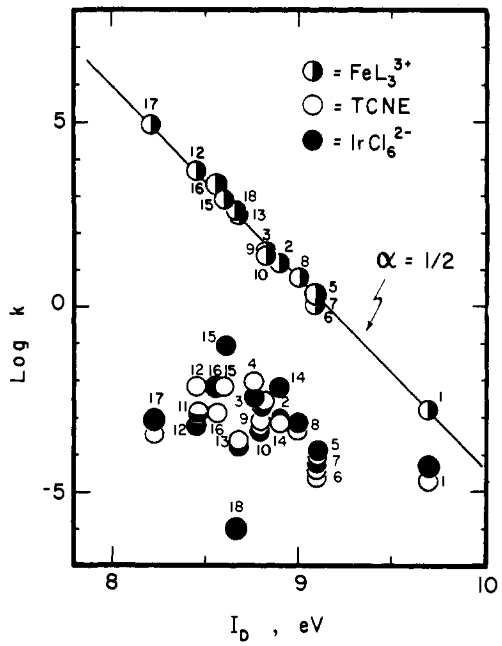

Figure 1. Relationship between the second-order rate constants for electron transfer to (◑) $Fe(phen)_3^{3+}$, (●) $IrCl_6^{2-}$, and (○) TCNE and the ionization potentials of tetraalkyltin identified by the numbers in Table II.

Table III. Selectivity Studies in the Oxidative Cleavage of Methylethyltin Compounds by $Fe(phen)_3^{3+}$, $IrCl_6^{2-}$, and TCNE[a]

alkyltin	oxidant/acceptor	$\mathcal{S}$(Et/Me)[b]
Me_2Et_2Sn	$Fe(phen)_3(ClO_4)_3$	27 ± 4
	Na_2IrCl_6	11 ± 3
	TCNE	10 ± 3
Me_3EtSn	$Fe(phen)_3(ClO_4)_3$	26 ± 4
	Na_2IrCl_6	11 ± 3
	TCNE	11 ± 3
$MeEt_3Sn$	$Fe(phen)_3(ClO_4)_3$	[c]
	Na_2IrCl_6	11 ± 3
	TCNE	[c]

[a] In acetonitrile solutions at 25 °C with 2 equiv of oxidant. [b] Selectivity is statistically corrected in Me_3EtSn and $MeEt_3Sn$. [c] Not measurable.

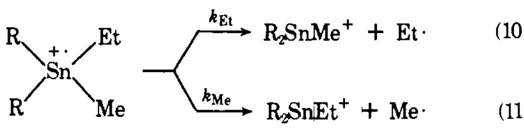

$$R_2Sn(Et)(Me)^{+\cdot} \xrightarrow{k_{Et}} R_2SnMe^+ + Et\cdot \quad (10)$$

$$R_2Sn(Et)(Me)^{+\cdot} \xrightarrow{k_{Me}} R_2SnEt^+ + Me\cdot \quad (11)$$

Selectivity provides the only measure available to determine the properties of the radical cation intermediate, $R_2SnMeEt^+$. Indeed, the grouping of $\mathcal{S}$(Et/Me) in Table III indicates that the cation derived from FeL_3^{3+} is different from those derived from $IrCl_6^{2-}$ and TCNE. Furthermore, the similar values of $\mathcal{S}$(Et/Me) for the latter accord with a common inner-sphere process. It is noteworthy that all of the selectivities with $\mathcal{S}(Et/Me) \gg 1$, including those obtained from mass spectral cracking patterns,[17] are quite distinct from those observed in electrophilic cleavage. For example, the electrophilic cleavage of methylethyllead compounds by acid [$\mathcal{S}$(Et/Me) = 0.11 and 0.021 for HOAc and H_2OAc^+, respectively] and metal ions [$\mathcal{S}$(Et/Me) = 0.018 and 0.022 for CuOAc and $CuCl_2$, respectively] all involve the *direct* bimolecular scission of the alkyl-metal bond by the electrophile.[20]

C. Activation Parameters for Electron Transfer. The temperature dependences of the second-order rate constants for electron transfer were determined for FeL_3^{3+}, $IrCl_6^{2-}$, and TCNE to obtain measures of the enthalpy of activation.[21] The series of tetraalkyltins are listed in Table IV more or less in the order of increasing steric bulk about the tin center (see Table I). The enthalpy of activation for FeL_3^{3+} is directly related to the ionization potential of the alkylmetal. Indeed the slope of the linear correlation for FeL_3^{3+} in Figure 2 is close to the Bronsted slope of $\alpha = 0.5$ in Figure 1, in accord with the Gibbs–Helmholtz equation.[22] It is noteworthy that the rates of electron transfer to TCNE are significantly less susceptible to changes in the ionization potential.

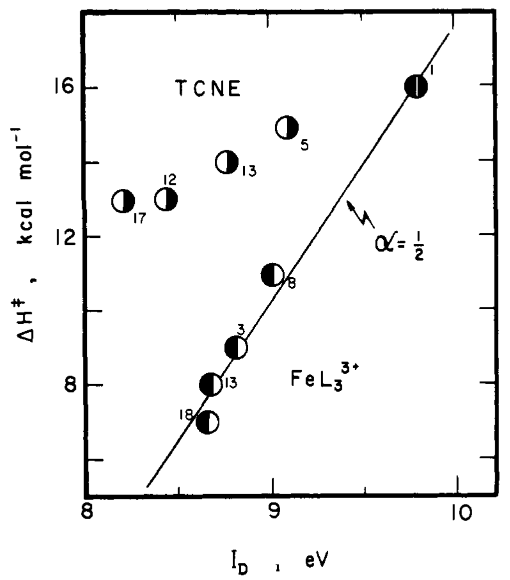

Figure 2. The correlation of the ionization potentials of tetraalkyltin with the enthalpy of activation for electron transfer to (◐) $Fe(4,7\text{-}Ph_2phen)_3^{3+}$ and (◑) TCNE. The line is drawn with Brønsted slope of $\alpha = \frac{1}{2}$.

II. Outer-Sphere and Inner-Sphere Mechanisms for Electron Transfer from Alkylmetals. Criteria Based on Steric Effects. In order to account for the contrasting behavior of FeL_3^{3+} relative to both $IrCl_6^{2-}$ and TCNE, we first rely on the Marcus theory to provide the quantitative basis for electron-transfer mechanisms, using the well-established free energy relationship:[1]

$$\Delta G^\ddagger = w_r + \frac{\lambda}{4}\left[1 + \frac{\Delta G}{\lambda}\right]^2 \qquad (12)$$

where $\Delta G = \Delta G^\circ + w_p - w_r$, and ΔG° is the standard free energy change accompanying electron transfer. The reorganization term λ corresponds to $4(\Delta G^\ddagger - w_r)$ at $\Delta G = 0$; w_r and w_p are the work terms required to bring the reactants and products, respectively, to their mean separation $r^\ddagger$ in the activated complex.

A. Outer-Sphere Mechanism for FeL_3^{3+}. The Marcus eq 12 is applicable to the outer-sphere mechanism for electron transfer when $|\Delta G| \leq \lambda$. In order to apply it to electron transfer from neutral alkylmetals RM to FeL_3^{3+} complexes, eq 12 can be rewritten in an alternative form as

$$\sqrt{\Delta G^\ddagger} = \left[\frac{\sqrt{\lambda}}{2} + \frac{\mathcal{F}}{2\sqrt{\lambda}}\left(E^\circ_{RM} + \frac{w_p}{\mathcal{F}}\right)\right] - \frac{\mathcal{F}}{2\sqrt{\lambda}}E^\circ_{Fe} \qquad (13)$$

since $\Delta G^\circ = \mathcal{F}(E^\circ_{RM} - E^\circ_{Fe})$ and $w_r = 0$. (E°_{RM} and E°_{Fe} are the standard electrode potentials of the alkylmetal and FeL_3^{3+}, respectively, and $\mathcal{F}$ is the Faraday constant.[23]) It is noteworthy that the correlation between $\sqrt{\Delta G^\ddagger}$ and E°_{Fe} is linear, as shown in Figure 3 (left) using the experimental values from Table II and our recent study.[12] Importantly, the slopes of these correlations $\mathcal{F}/2\sqrt{\lambda}$ are constant for alkylmetals spanning the range from tetramethyltin to the highly hindered tetraneopentyltin. Thus the reorganization energies for all of these alkylmetals are the same, independent of their steric bulk, and given by[24]

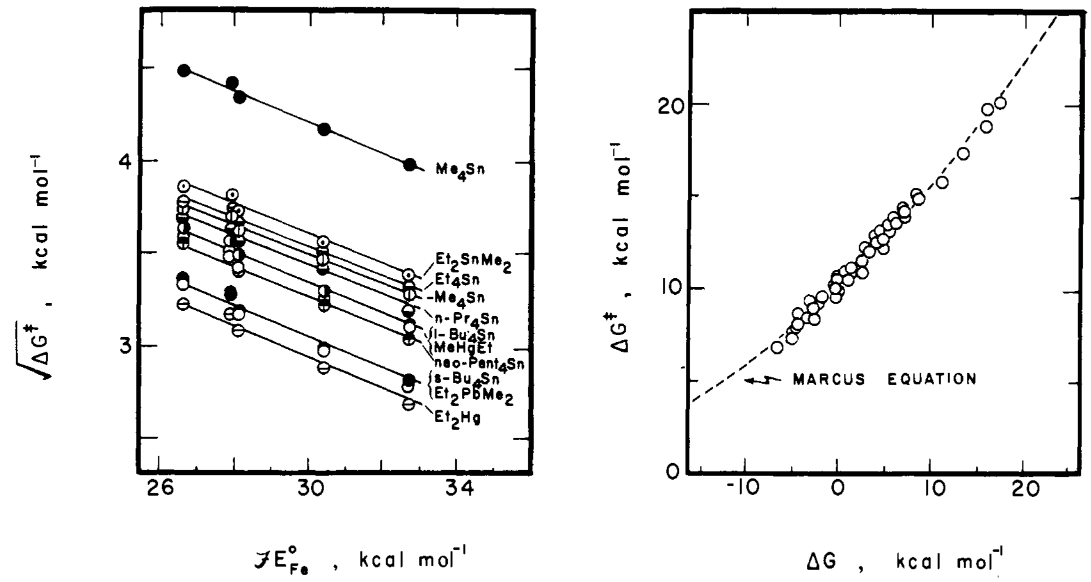

Figure 3. The relationship of the activation free energy for electron transfer with (left) the electrode potentials of various FeL_3^{3+} complexes according to eq 13 and (right) the driving force according to eq 12.

Table IV. Temperature Dependence of the Second-Order Rate Constants for Electron Transfer to $Fe(4,7\text{-}Ph_2phen)_3^{3+}$, $IrCl_6^{2-}$, and TCNE from Tetraalkyltin[a]

SnR_4	k_{25}	$k_{43.5}$	k_{50}	k_{58}	k_{70}	$\Delta H^{\ddagger}$, kcal mol⁻¹
			$IrCl_6^{2-}$			
Me_4Sn	5.2×10^{-5}		6.6×10^{-4}		5.1×10^{-3}	20 ± 2
$EtSnMe_3$	1.4×10^{-4}	7.8×10^{-4}		3.0×10^{-3}		18 ± 1
t-Bu_2SnMe_2	9.4×10^{-4}		3.7×10^{-3}		1.1×10^{-2}	10 ± 2
i-Bu_4Sn	1.4×10^{-4}		4.6×10^{-4}		1.5×10^{-3}	10 ± 3
sec-Bu_4Sn	5.9×10^{-4}	1.4×10^{-3}		3.1×10^{-3}		9 ± 2
neo-$Pent_3SnEt$	1.9×10^{-5}	4.9×10^{-5}		1.1×10^{-4}		10 ± 2
			TCNE			
Me_4Sn	1.5×10^{-5}	7.0×10^{-5}	1.1×10^{-4}		6.6×10^{-4}	16 ± 2
$EtSnMe_3$	9.2×10^{-5}	3.8×10^{-4}		1.2×10^{-3}		15 ± 3
t-Bu_2SnMe_2	3.7×10^{-4}	1.3×10^{-3}	1.9×10^{-3}		7.5×10^{-3}	13 ± 2
i-Bu_4Sn	2.2×10^{-4}		1.4×10^{-3}		5.7×10^{-3}	14 ± 3
sec-Bu_4Sn	6.1×10^{-3}		2.1×10^{-2}		5.8×10^{-2}	13 ± 3

SnR_4	k_0	k_{25}	$k_{35.5}$	k_{50}	$\Delta H^{\ddagger}$, kcal mol⁻¹
		$Fe(4,7\text{-}diPh_2phen)_3(ClO_4)_3$			
Me_4Sn		1.7×10^{-4}	4.5×10^{-4}	1.5×10^{-3}	16 ± 1
Et_2SnMe_2	0.21	1.2	2.2		11 ± 1
n-Pr_4Sn	2.4	11	18		9 ± 2
i-Bu_4Sn	11	43.0	72		8 ± 2
neo-$Pent_4Sn$	15	52	82		7 ± 2

[a] Second-order rate constant in $M^{-1}\,s^{-1}$ in acetonitrile solutions. Subscripts refer to temperature in °C.

$$\lambda = 41 \pm 3 \text{ kcal mol}^{-1} \qquad (14)$$

The magnitude of the driving force derived from the alkylmetal, i.e., $\mathcal{F}E°_{RM} + w_p$, can be obtained from the intercepts in Figure 3 together with λ from eq 14, and they are listed in the Experimental Section.

The activation free energies $\Delta G^{\ddagger}$ obtained from the kinetic data are plotted against the driving force ΔG in Figure 3 (right). The dashed line in the figure represents $\Delta G^{\ddagger}$ calculated from eq 12 with λ from eq 14. The agreement is the same as that shown on the left figure, but it encompasses all 63 experimental points and covers a span of more than 20 kcal mol⁻¹. Thus electron transfer from alkylmetals to FeL_3^{3+} accords well with the Marcus theory for outer-sphere mechanisms. The absence of notable steric effects must be emphasized.

B. Inner-Sphere Mechanism for TCNE and $IrCl_6^{2-}$. In contrast to FeL_3^{3+}, the rates of electron transfer to TCNE and $IrCl_6^{2-}$ do not follow a smooth correlation with the driving force. In Figure 4, the experimental values of $\Delta G^{\ddagger}$ for TCNE (left) and $IrCl_6^{2-}$ (right) consistently fall below the solid lines representing the correlation of the outer-sphere rates described in the foregoing section (taking into account differences in reorganization energies of $IrCl_6^{2-}$ and TCNE[25]). With the exception of *t*-Bu_2SnMe_2, *all the experimental rates are faster than the calculated values based on the Marcus outer-sphere correlation.*[26] The magnitudes of the deviation vary from 12.5 kcal mol⁻¹ for Me_4Sn (which corresponds to an increase by a factor of more than 10^9 in rates) to ~0 for *t*-Bu_2SnMe_2. A close scrutiny of the data reveals that the deviations from the outer-sphere correlation are the most pronounced with the least hindered alkylmetals. Thus, among the symmetrical tetraal-

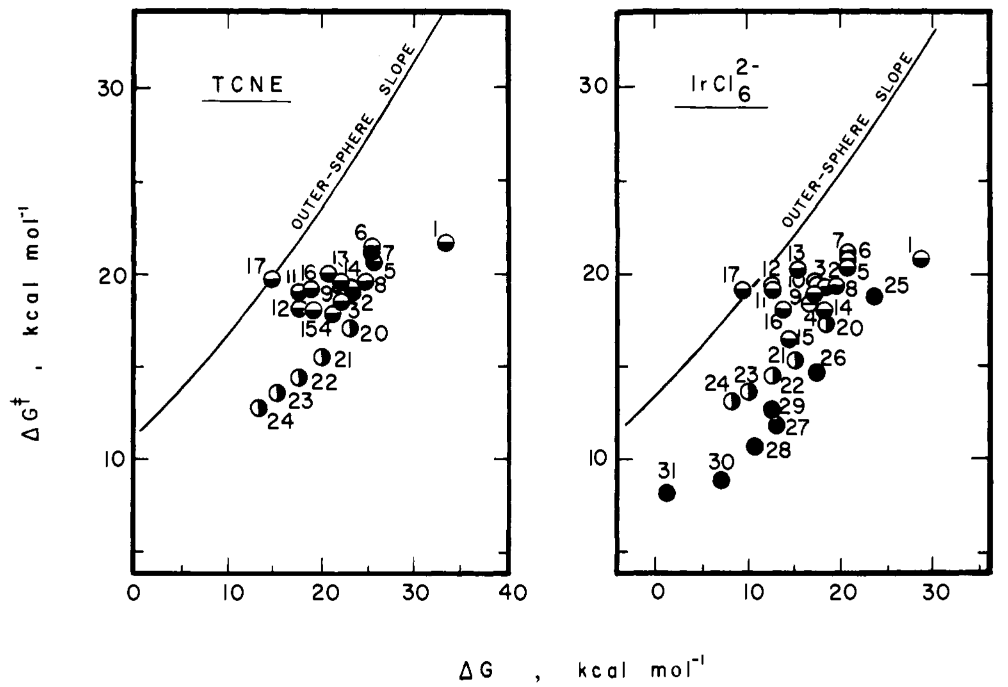

Figure 4. The relationship between the activation free energy and the driving force for electron transfer from alkylmetals to TCNE (left) and $IrCl_6^{2-}$ (right) according to Marcus eq 12. Numbers refer to alkylmetals R_nM in Tables II and VI, where M = Sn (⊖), Pb (◑), and Hg (●).

kyltin compounds R_4Sn, the least hindered methyl and the straight-chain *n*-alkyl derivatives all lie farthest from the outer-sphere correlation. Conversely, those tetraalkyltin compounds with α- and β-branched alkyl ligands (i.e., isopropyl, isobutyl, *sec*-butyl, and *tert*-butyl) consistently lie closest to the dashed lines in Figure 4. Furthermore, the two-coordinate dialkylmercurials, which represent sterically open alkylmetals, all lie away from the outer-sphere correlation, significantly beyond the *n*-alkyltin derivatives. Such a trend must reflect steric effects which perturb the inner coordination sphere of the alkylmetal in the transition state for electron transfer to TCNE and $IrCl_6^{2-}$. Indeed, we wish to employ this conclusion as an operational definition for an inner-sphere mechanism of electron transfer from alkylmetals.

In the context of the Marcus formulation, the lowering of the activation barrier in an inner-sphere process could arise from the reduction of the work term w_p as a result of the strong interaction in the ionic products, viz., $[R_4Sn^{+}\cdot TCNE^{-}\cdot]$ and $[R_4Sn^{+}\cdot IrCl_6^{3-}]$.[27,28] The electrostatic potential in such ion pairs is attractive, and may cause the tetraalkyltin to achieve a quasi-five-coordinate configuration in the precursor complex, reminiscent of a variety of trigonal-bipyramidal structures known for tin(IV) derivatives, i.e.

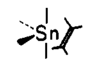

A

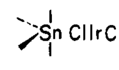

B

The extent to which steric effects adversely affect the attainment of such intimate ion-pair structures would be reflected in an increase in the work term and concomitant diminution of the inner-sphere rate [27,29] This qualitative conclusion accords with the trends in Figure 5. However, Marcus theory does not provide a *quantitative* basis for evaluating the variation in the work term of such ion pairs. To obtain the latter, we now turn to the Mulliken theory of charge transfer in which the energetics of ion-pair formation evolve directly, and provide quantitative information on the steric effects.

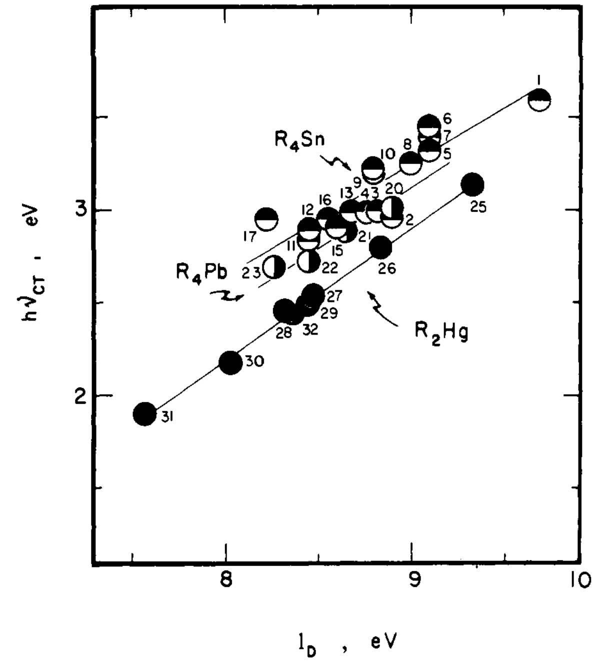

Figure 5. The relationship between the ionization potentials of alkylmetals [(●) dialkylmercury, (⊖) tetraalkyltin, and (◑) methylethyllead] and the charge-transfer frequencies of TCNE complexes. Numbers refer to alkylmetals in Tables II and V.

III. Quantitative Evaluation of Steric Effects of Alkylmetals in Inner-Sphere Electron Transfer. The new absorption bands observed in the visible region immediately upon mixing TCNE with solutions of various alkyltin compounds are due to charge-transfer complexes, i.e.[17]

$$R_4Sn + TCNE \rightleftharpoons [R_4Sn\ TCNE] \tag{6}$$

According to Mulliken charge transfer theory, the spectral transition $h\nu_{CT}$ represents an electronic excitation from the ground state Ψ_N of the complex to the excited state Ψ_E.[3] For weak complexes of the type described here for alkylmetals and TCNE, this transition occurs essentially from the structure $\Psi_0(RM\ TCNE)$ to the structure $\Psi_1(RM^{+}\cdot TCNE^{-}\cdot)$; i.e., it corresponds to an intermolecular transition within the complex

Table V. Evaluation of Steric Effects from the Charge-Transfer Interaction of Alkyltin with TCNE. Relationship of Electron Transfer to $IrCl_6^{2-}$ [a]

R_4M	ν_{CT},[a] eV	K_{CT},[a] M^{-1}	ΔE, kcal mol^{-1}	log k_{TCNE}	log k_{TCNE}^{cor} [c]	log k_{Ir}	log k_{Ir}^{cor} [c]
Me_4Sn	3.59	0.17	0	−4.82	−4.82	−4.29	−4.29
Et_4Sn	2.95	0.53	3.5	−3.07	−0.53	−3.20	−0.66
n-Pr_4Sn	2.99	2.2	6.2	−2.59	1.97	−3.34	1.22
n-Bu_4Sn	2.98	7.7	7.4	−2.04	3.37	−2.49	2.92
$EtSnMe_3$	3.32	0.24	7.4	−4.04	1.37	−3.87	1.54
n-$PrSnMe_3$	3.45	0.25	10.4	−4.70	2.91	−4.28	3.33
n-$BuSnMe_3$	3.40	0.21	9.2	−4.54	2.22	−4.52	2.24
Et_2SnMe_2	3.25	0.80	7.8	−3.34	2.41	−3.16	2.59
n-Pr_2SnMe_2	3.20	1.5	11.5	−3.37	5.08	−2.89	5.56
n-Bu_2SnMe_2	3.21	1.1	11.8	−3.20	5.42	−3.44	5.18
i-Pr_4Sn	2.83	1.0	10.8	−2.85	5.09	−3.00	4.94
sec-Bu_4Sn	2.89	2.5	12.5	−2.21	6.92	−3.23	5.90
i-Bu_4Sn	2.99	0.30	9.5	−3.66	3.27	−3.86	3.07
i-$PrSnMe_3$	3.06	1.0	6.0	−3.19	1.20	−2.19	2.20
t-$BuSnMe_3$	2.91		9.5	−2.18	4.75	−1.11	5.82
i-Pr_2SnMe_2	2.95	0.95	11.3	−2.92	5.36	−2.19	6.09
t-Bu_2SnMe_2	2.95	0.65	19.1	−3.43	10.57	−3.02	10.98
i-Bu_2SnEt_2	2.95	0.40		−3.48			
Et_3SnMe	3.02						

[a] Charge-transfer data in chloroform solution at 25 °C from ref 17. [b] Calculated from eq 17. [c] Calculated from eq 21.

Table VI. Correction for Steric Effects in Electron Transfer from Methylethyllead and Dialkylmercury Compounds to TCNE and $IrCl_6^{2-}$ [a]

no.	RM	I_D, eV	ν_{CT}, eV	ΔE,[b] kcal mol^{-1}	log k_{TCNE}	log k_{TCNE}^{cor} [c]	log k_{Ir}	log k_{Ir}^{cor} [c]
20	Me_4Pb	8.90	3.01	4.8	−1.50	2.05	−1.70	1.85
21	$EtPbMe_3$	8.65	2.89	7.8	−0.28	5.47	−0.24	5.51
22	Et_2PbMe_2	8.45	2.73	8.8	0.49	6.91	0.52	6.94
23	Et_3PbMe	8.26	2.59	9.9	1.08	8.35	1.04	8.31
24	Et_4Pb	8.13			1.68		1.41	
25	Me_2Hg	9.33	3.14	−2.1			−2.82	−4.34
26	$EtHgMe$	8.84	2.79	1.2			0.30	1.15
27	*i*-$PrHgMe$	8.48	2.53	3.5			2.34	4.88
28	*t*-$BuHgMe$	8.31	2.45	5.5			3.20	7.26
29	Et_2Hg	8.45	2.48	3.0			1.68	3.88
30	*i*-Pr_2Hg	8.03	2.17	5.5			4.52	8.58
31	*t*-Bu_2Hg	7.57	1.90	9.9			4.96	12.23
32	*n*-Bu_2Hg	8.35	2.44					
33	Et_4Ge	9.41	3.35[d]	0.9			−4.83	−4.15

[a] Data from ref 13 and 16, unless stated otherwise. [b] Calculated from eq 17. [c] Calculated from eq 21. [d] From ref 10b.

involving electron transfer from RM to TCNE, as represented by

$$[\mathrm{RM\ TCNE}] \xrightarrow{h\nu_{CT}} [\mathrm{RM^{+}\cdot TCNE^{-}\cdot}]^{*} \qquad (15)$$

The asterisk identifies an excited ion pair with the same mean separation r_{DA} as that in the CT complex; i.e., eq 15 represents a vertical (Franck-Condon) transition, the energy of which is given by

$$h\nu_{CT} = I_D + E_A + \omega \qquad (16)$$

The interaction energy ω of the excited ion pair includes the electrostatic work term ($-e^2/r_{DA}$), the resonance interaction, etc. (compare eq 9).[3,30,31] In a recent study,[19] we showed that ω can vary in a series of alkylmetal CT complexes as a result of changes in the steric properties of the alkyl ligands. Thus the variations in the CT transition energies when plotted against I_D are shown by a family of lines in Figure 5 for alkyltin, -lead, and -mercury. The separate correlations for each indicate that the interaction energies in these CT complexes decrease in the order $R_2Hg \gg R_4Pb > R_4Sn$. Furthermore, the separations among various alkylmetals are highly reminiscent of the changes in the work terms of the thermally formed ion pairs **A** and **B** in Figure 4. In other words, the scatter of points in Figure 5 should be related to the variations in $\Delta G^{\ddagger}$ from the correlation in Figure 4.

In order to carry out this evaluation quantitatively, we relate ω for various tetraalkyltin to ω_0 of the least sterically hindered Me_4Sn, chosen as a reference. It follows from eq 16 that the energy change, $\Delta E = \omega - \omega_0$, is given by

$$\Delta E = -\Delta I_D + \Delta h\nu_{CT} \qquad (17)$$

where ΔI_D is the difference in the ionization potentials between a particular tetraalkyltin and Me_4Sn, and $\Delta h\nu_{CT}$ is the difference in their CT energies in the TCNE complexes. Thus *by choosing a reference alkylmetal, all changes in the interaction energies of these CT complexes, including steric, distortional, and other effects, can be compositely expressed in a single energy term* ΔE.[32] Hereafter we arbitrarily refer to ΔE as the steric term, which can be directly obtained from the experimental data according to eq 17. The values of ΔE are listed in Tables V and VI.

We now return to the thermal reaction as it proceeds from the CT complex described in Scheme III, in which the rate-limiting activation process has been shown to be electron transfer, i.e.[17]

$$[\mathrm{RM\ TCNE}] \xrightarrow{k} [\mathrm{RM^{+}\cdot TCNE^{-}\cdot}] \qquad (18)$$

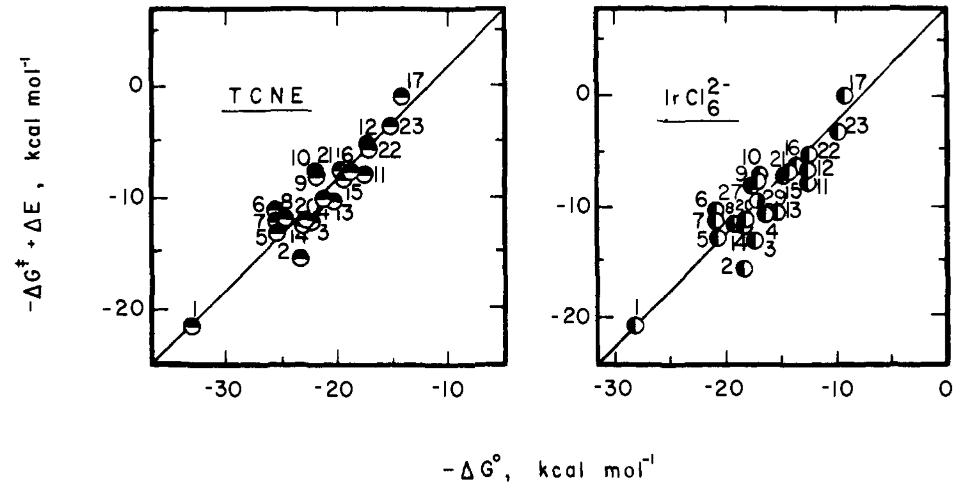

Figure 6. The relationship between the activation free energy ($\Delta G^{\ddagger}$) including the steric term (ΔE) and the driving force for electron transfer (ΔG°) to TCNE (left) and $IrCl_6^{2-}$ (right), assuming w in eq 20 to be negligible. Numbers refer to alkylmetals in Table II. The lines are drawn with a Brønsted slope of $\alpha = 1$.

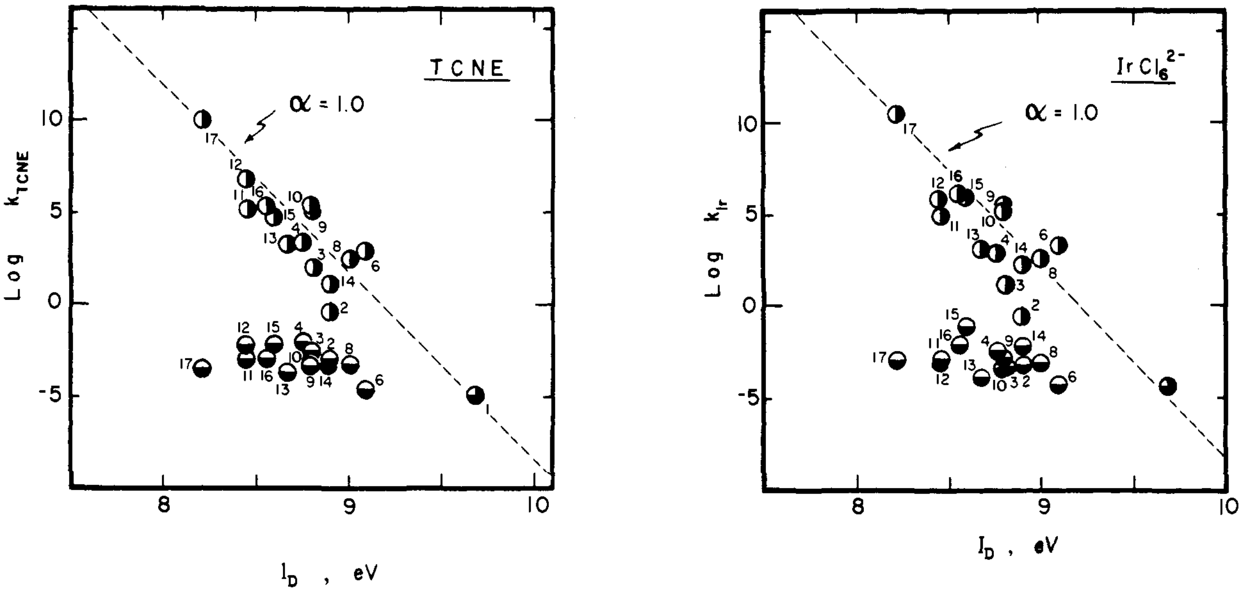

Figure 7. The linear free energy relationship of the electron-transfer rate constant from tetraalkyltin to TCNE (left) and $IrCl_6^{2-}$ (right): (◒) before and (◑) after correction for steric effects according to eq 21. Numbers refer to tetraalkyltin in Table II. See text for dashed line which is arbitrarily drawn with Brønsted slope of $\alpha = 1$.

Since the relative reactivities of alkylmetals are our primary concern, the changes in the free-energy terms for electron transfer can be related to a reference alkylmetal (hereafter indicated by the subscript zero) by a procedure similar to that described above. Accordingly, the variation in the *driving force* for electron transfer from various alkylmetals in eq 18 derives from two factors: (1) the differences in the oxidation potentials of the alkylmetals and (2) the changes in the interaction energies in the thermal ion pairs. The first is obtained from the free-energy change ΔG° for electron transfer, i.e., $RM \rightarrow RM^{+}\cdot$ in the outer-sphere process (see eq 12 or 13). The change in the interaction energy is equated to ΔE, determined from the CT complexes in eq 17, since the thermally formed ion pair $[RM^{+}\cdot TCNE^{-}\cdot]$ in eq 18 is akin to the photochemically excited ion pair $[RM^{+}\cdot TCNE^{-}\cdot]^{*}$ in eq 15.[33]

The change in the *activation free energy* $\Delta G^{\ddagger}$ for electron transfer to various alkylmetals may be evaluated by a similar comparative procedure, i.e.

$$\Delta G^{\ddagger} - \Delta G_0^{\ddagger} = -2.3RT \log k/k_0 \qquad (19)$$

where k and k_0 are the rates of electron transfer in $[R_4M\ TCNE]$ and $[Me_4Sn\ TCNE]$, respectively.

The striking linear correlation in Figure 6 (left) between the driving force and the activation free energy represents a linear free energy relationship for electron transfer to TCNE expressed as

$$\Delta G^{\ddagger} = \Delta G^{\circ} + \Delta E + C \qquad (20)$$

where the constant $C = \Delta G_0^{\ddagger} - \Delta G_0^{\circ} + w$. ($w$ is the outer-sphere work term for FeL_3^{3+}.) Furthermore, the same relationship applies to $IrCl_6^{2-}$ as shown by the correlation in Figure 6 (right).

Since the Brønsted slope in eq 20 is unity, the steric term $\Delta E/2.3RT$ can also be considered as a correction factor $\Delta \log k$ on the rates of electron transfer, i.e.

$$\log k^{cor} = \log k + (\Delta E/2.3RT) \qquad (21)$$

where k is the experimental rate constant. Under these circumstances, $\log k^{cor}$ in column 6 of Table V represents the electron transfer rate constant under hypothetical conditions of constant steric effects (i.e., relative to that of the chosen reference Me_4Sn). Stated alternatively, $\log k^{cor}$, or its equivalent $\Delta G^{\ddagger} - \Delta E$, is the form to be related to the driving force of the electron transfer (ΔG°), in the absence of steric effects. Figure 7 (left) shows the new correlation of the data previously presented in Figure 1 for the electron transfer rate constants

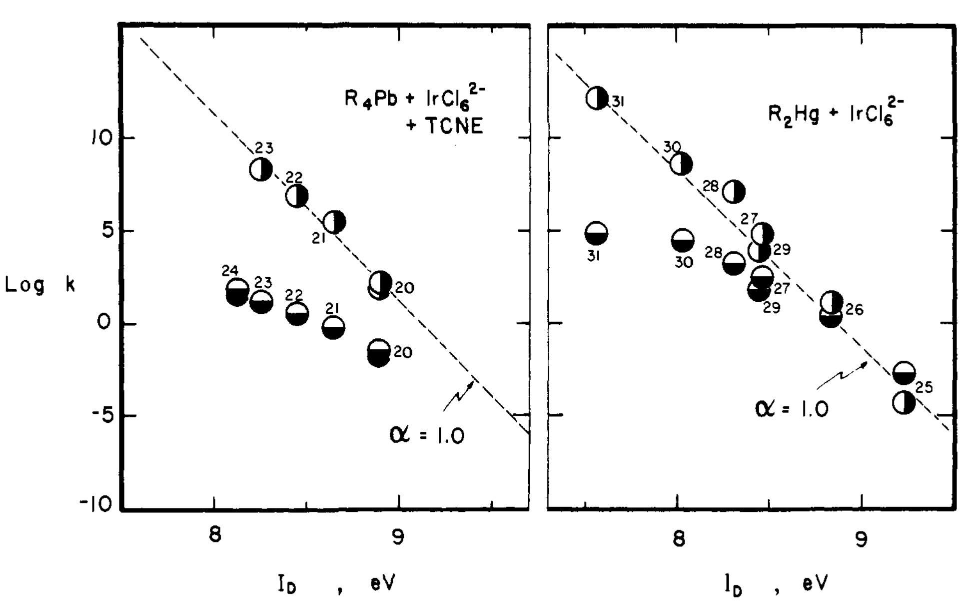

Figure 8. The linear free energy relationship of the electron-transfer rate constants for methylethyllead compounds with TCNE and $IrCl_6^{2-}$ (left) and dialkylmercury with $IrCl_6^{2-}$ (right): (◒) before and (◑) after correction for steric effects. Numbers refer to alkylmetals in Table VI.

between TCNE and a series of tetraalkyltin compounds. The dashed line in Figure 7 is arbitrarily drawn with a Bronsted slope of $\alpha = 1$[34] through the point for Me_4Sn, and it shows a reasonable agreement with the values of log k^{cor} determined from eq 21. The same correction applied to the rates of electron transfer to $IrCl_6^{2-}$ is shown in Figure 7 (right).[35]

The second-order rate constants for electron transfer from the complete series of methylethyllead compounds to hexachloroiridate(IV) and tetracyanoethylene were reported in earlier studies.[13,16] The rate constants for TCNE and $IrCl_6^{2-}$, before and after the steric correction, are listed in Table VI. It is noteworthy that the points for log k^{cor} of both TCNE and $IrCl_6^{2-}$ in Figure 8 (left) fall precisely on the dashed line, arbitrarily drawn with a Brønsted slope of one. (The displacement of the dashed line above the experimental point for Me_4Pb results from the use of Me_4Sn as the reference in eq 17. The amount of displacement includes a contribution from the differences in ω between Me_4Pb and Me_4Sn in eq 16.) Similarly, for a variety of dialkylmercury compounds, the linear free energy plot of the experimental second-order rate constants in Figure 8 (right) shows considerable deviation from linearity. However, after correction by an amount Δ log k, the values of log k^{cor} are well correlated by a dashed line drawn with a Bronsted slope of one. (The displacement of the dashed line below the experimental point for Me_2Hg results from the use of Me_4Sn in eq 17.)

It is striking that all of the diverse rate data for electron transfer from various alkylmetals to TCNE and $IrCl_6^{2-}$ after the steric correction uniformly fall on a *single* linear correlation with a Brønsted slope of unity. [It is important to point out that the linear free energy relationship in eq 20 (or its kinetic equivalent in eq 21) derives directly from the experimental data by a purely operational approach.] Essentially the same relationship has been predicted by Marcus for one extreme of an inner-sphere mechanism, where $\Delta G^\circ \geq \lambda$ (i.e., endergonic processes):[36]

$$\Delta G^{\ddagger} = \Delta G^\circ + w_p \qquad (22)$$

The Brønsted slope of $\alpha = 1$ in both expressions indicates that the activation processes for electron transfer from alkylmetals to TCNE and $IrCl_6^{2-}$ are accurately represented by the driving force for ion-pair formation.[37] As such, we now inquire as to which factors are important in delineating the intrinsic difference between the outer-sphere and inner-sphere mechanisms for electron transfer. Finally we wish to present a unified view of Marcus electron transfer and Mulliken charge transfer theories as they relate to this question.

IV. Comparison of Outer-Sphere and Inner-Sphere Mechanisms for Electron Transfer from Alkylmetals. The concepts of outer-sphere and inner-sphere electron transfer as we have employed in this study depend on the availability of various metals and alkyl ligands as highly tunable probes for steric effects. As such, we might ask how these mechanisms basically differ. One answer might focus on the properties of $RM^{+}\cdot$, especially with respect to selectivity in the subsequent cleavage, following the rate-limiting electron transfer. Another might relate to the role of steric effects on the activation process. We suggest that both are directly related to the interaction energy in the ion pair, for which steric effects are evaluated from the CT data by eq 17. According to this formulation, outer-sphere and inner-sphere processes are largely distinguished by the magnitudes of the intermolecular separation between the alkylmetal and the oxidant (acceptor) in the transition states for electron transfer. As such, there should be a continuum of activated complexes differing principally in geometrical constraints, which are manifested in the context of Marcus theory by variations in the work term as well as the reorganization energy.[27] In order to evaluate these contributions, let us see how they affect the free-energy correlations for outer-sphere (FeL_3^{3+}) and inner-sphere (TCNE and $IrCl_6^{2-}$) mechanisms illustrated in Figures 3 and 6, respectively. For clarity, these correlations are redrawn and juxtaposed in Figure 9.[38] (Note that the Brønsted slope for FeL_3^{3+} is effectively one-half, whereas that for both TCNE and $IrCl_6^{2-}$ is unity.) Initially, if the work term w_p in the Marcus eq 12 is reduced by $\Delta w_p \simeq$ 10 kcal mol^{-1}, the new free-energy correlation follows the dashed curve *a* in Figure 9. Following this, if the reorganization energy λ is reduced by one-half, curve *a* is transformed to *b*, which closely follows the inner-sphere correlation. Although the choice of Δw_p and $\lambda/2$ may appear arbitrary,[38,40] the procedure shows that the outer-sphere correlation can be transformed into the inner-sphere correlation by suitable reductions in the work term and reorganization energy. Since the experimental points in Figure 4 fall between the outer- and inner-sphere limits, it is reasonable to expect that variations in w_p and λ_{RM} lead to a continuum of inner-sphere and outer-sphere mechanisms. Thus, the least hindered Me_4Sn and the highly hindered t-Bu_2SnMe_2 expectedly lie at opposite extremes of the inner- and outer-sphere limits, respectively, as depicted for both TCNE and $IrCl_6^{2-}$ in Figure 4.

Table VII. Enthalpy of Formation of Selected Alkylmetal-TCNE Charge Transfer Complexes[a]

R_4M	K_{CT}, M^{-1} [b]	$-\Delta H_{CT}$, kcal mol^{-1}
Et_4Sn	0.53	0.9 ± 0.3
n-Pr_4Sn	2.2	1.5 ± 0.5
i-Bu_2SnEt_2	0.40	0.7 ± 0.3
n-$BuSnMe_3$	0.21	0.5 ± 0.3

[a] In chloroform solution. [b] 25 °C.

Summary and Conclusions

Organometals RM can be made to exhibit a wide range of steric and electron-donor properties by the judicious choice of alkyl ligands in Table I. A variety of four-coordinate tin, lead, germanium, and silicon alkyls, as well as two-coordinate dialkylmercury, are readily cleaved by tris(1,10-phenanthroline)iron(III), hexachloroiridate(IV), and tetracyanoethylene in a rate-limiting electron-transfer reaction. With tetracyanoethylene, an intermolecular charge-transfer complex [TCNE RM] can be detected as an intermediate, and its formation constant K_{CT} can be measured together with the charge-transfer transition $h\nu_{CT}$ in the electronic spectrum.

The rates of electron transfer from RM to tris(1,10-phenanthroline)iron(III) follow the Marcus linear free energy correlation in eq 12 with the predicted Bronsted slope $\alpha = 0.5$ for an outer-sphere mechanism. However, there is a uniform scatter of points in the same plot for hexachloroiridate(IV) and tetracyanoethylene, and the deviations are in accord with steric hindrance in RM. An inner-sphere mechanism for both $IrCl_6^{2-}$ and TCNE is also indicated by the rates of electron transfer, which are 10^{7-9} times faster than those predicted in eq 12. Separate mechanisms are also consistent with the differences in the selectivity S(Et/Me) of the cleavage of methylethyltin compounds and the activation parameters for electron transfer shown by FeL_3^{3+} in comparison with TCNE and $IrCl_6^{2-}$.

The steric effect in inner-sphere electron transfer can be quantitatively evaluated from changes ΔE in the charge transfer transition energies in eq 17, leading to the free-energy relationship $\Delta G^{\ddagger} = \Delta G° + \Delta E$ + constant in eq 20.

In the region of weak overlap as in outer-sphere mechanisms, the Marcus eq 12 successfully provides a theoretical basis for predicting electron-transfer rates, as we have shown in Figure 3 for alkylmetals with FeL_3^{3+} complexes. If the same formulation is applied directly to the inner-sphere electron transfer with TCNE and $IrCl_6^{2-}$, a large reduction in the work term is necessitated in order to accommodate rates which can be many orders of magnitude faster than those predicted by eq 12. This change in the work term as a result of steric hindrance is functionally equivalent to the change in the interaction energy ΔE of the ion pair when comparisons are made relative to a reference alkylmetal. Indeed, ΔE derived from the CT transition energy in eq 17 is in striking agreement with relative values of w_p based on the Marcus eq 22. In other words, the unification of the Marcus electron transfer and the Mulliken charge transfer theories provides a quantitative basis for predicting the rates of inner-sphere electron transfer with alkylmetals. Individually, neither is adequate since the work term is no longer constant for inner-sphere mechanisms in the Marcus theory, and Mulliken theory itself provides no direct relationship with electron-transfer reactions. Finally, the close parallel between the classic inorganic oxidant $IrCl_6^{2-}$ and the classic organic acceptor TCNE forcefully demonstrates the need to consider electron-transfer and charge-transfer processes from a single, unified view.

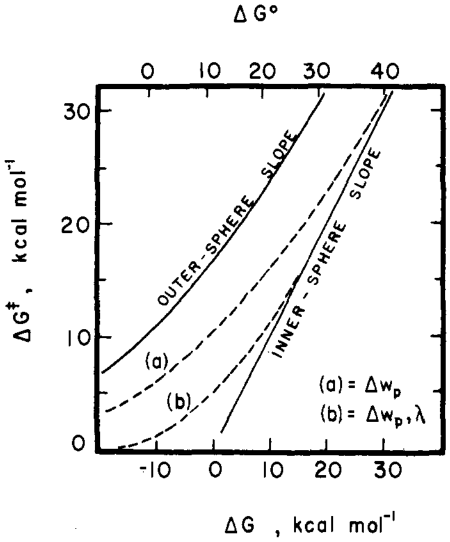

Figure 9. The importance of the work term and the reorganization energy in the free energy correlations for outer-sphere (upper scale[39]) and inner-sphere (lower scale) mechanisms as described in the text.

Experimental Section

The materials used in this study have been previously described.[12,17]

Charge-Transfer Spectra of Alkyltin Compounds and TCNE. A solution of 0.01 M TCNE in chloroform contained in a 10-mm quartz cuvette was equilibrated in a thermostated compartment of a Cary 14 spectrophotometer. The alkyltin compound (5–400 μL) was added by means of a microsyringe and rapidly mixed. With most alkyltin, the absorption spectrum measurably decreased within a few minutes and necessitated rapid measurement of the spectrum. However, reproducibility to within 5% could be readily achieved. The temperature dependence studies were carried out at 0, 25, and 35 °C. The formation constants in Table VII were calculated assuming that the extinction coefficients[17] are temperature independent. The formation constants K_{CT}, measured spectrophotometrically, are uniformly rather small. These charge-transfer complexes are classified as very weak, which is to be expected from symmetry considerations of limited orbital overlap between a π acceptor such as TCNE and alkylmetals acting as σ donors. The small values of the heats of formation ΔH_{CT}

Table VIII. Oxidation Potentials of Alkylmetals[a]

RM	$E°_{RM} + (w_p/\mathcal{F})$	RM	$E°_{RM} + (w_p/\mathcal{F})$	RM	$E°_{RM} + (w_p/\mathcal{F})$
Me_4Sn	1.90	*i*-Pr_4Sn	1.22	Et_2PbMe_2	1.21
Et_4Sn	1.46	*sec*-Bu_4Sn	1.21	Et_3PbMe	1.11[b]
n-Pr_4Sn	1.42	*i*-Bu_4Sn	1.34	Et_4Pb	1.03
n-Bu_4Sn	1.38	*i*-$PrSnMe_3$	1.46[b]	Me_2Hg	1.70[b]
$EtSnMe_3$	1.57[b]	*t*-$BuSnMe_3$	1.29	$EtHgMe$	1.43
n-$PrSnMe_3$	1.57	*i*-Pr_2SnMe_2	1.27	*i*-$PrHgMe$	1.23[b]
n-$BuSnMe_3$	1.57	*t*-Bu_2SnMe_2	1.08	*t*-$BuHgMe$	1.13[b]
Et_2SnMe_2	1.52	*neo*-$Pent_4Sn$	1.33	Et_2Hg	1.21
n-Pr_2SnMe_2	1.41	Me_4Pb	1.46	*i*-Pr_2Hg	0.98[b]
n-Bu_2SnMe_2	1.41	$EtPbMe_3$	1.32[b]	*t*-Bu_2Hg	0.72[b]

[a] Volts vs. SHE including the work term w_p for electron transfer to FeL_3^{3+}. [b] Extrapolated values based on the relationship with I_D (see ref 34).

in Table VII, obtained from temperature-dependence studies, indicate that the resonance stabilization term [$\sim -2\Delta H_{CT}$] in eq 9 obtained from the second-order perturbation treatment is negligible for these very weak complexes.

Kinetic Measurements. Tris(phenanthroline)iron(III) and Hexachloroiridate(IV). Solutions of alkylmetal in acetonitrile were purged with argon and used within 2 days of preparation. Solutions of iron(III) complexes were freshly prepared in deaerated acetonitrile. Whenever possible, the reactions were carried out under pseudo-first-order conditions with either the alkylmetal or the iron(III) complex in excess. For the slower reactions, the appropriate concentrations of alkylmetal and iron(III) complex were made up in pre-deaerated acetonitrile and subsequently transferred to a gas-tight Pyrex cuvette in a thermostated cell compartment of a Cary 14 spectrophotometer. The rate of disappearance of hexachloroiridate(IV) was followed at 489 nm. For oxidations with iron(III), the rate of appearance of the band due to the corresponding iron(II) complex was followed, i.e., $Fe(phen)_3^{2+}$, 510 nm (ϵ 1.30 × 10^4), and $Fe(4,7\text{-}Ph_2phen)_3^{2+}$, 510 nm ($\epsilon$ 1.26 × 10^4). The ionic strength of the reaction medium was adjusted to 0.1 with either lithium perchlorate or tetraethylammonium perchlorate. For reactions which were too fast to be followed by this procedure, separate solutions of the alkylmetal and the iron(III) complex were sealed in conical flasks with serum caps and purged with argon. The resulting reagents were transferred by means of glass syringes to a Durrum-Gibson stopped-flow spectrophotometer.

Tetracyanoethylene. A 10-mm cuvette containing a solution of 10^{-4} M TCNE in acetonitrile was placed in a thermostated compartment of a Cary 14 spectrophotometer. The reaction was started by injecting 2–100 μL of tetraalkyltin (corresponding to 10^{-2} M) by means of a microsyringe with shaking. The decrease in TCNE absorbance at 270.5 nm (ϵ 15 500) was followed. Tetraalkyltin used in this study does not absorb in this region. Similar results could be obtained with the less reactive alkyltin compounds by observing the changes in the ^{1}H NMR spectra as described in more detail for the selectivity studies below.

Selectivity Studies with Methylethyltin Compounds. The determination of selectivities in the insertion of TCNE into alkylmetals has been described.[17] The selectivity in the cleavage of alkylmetals by FeL_3^{3+} and $IrCl_6^{2-}$ is described in ref 12.

Evaluation of Oxidation Potentials of Alkylmetals from the Marcus Equation. Attempts to measure directly the reversible oxidation potentials of the alkylmetals in acetronitrile solutions by either cyclic voltammetry or ac polarography were unsuccessful, since the voltammograms were irreversible even at scan rates as high as 10 V s^{-1} and temperatures as low as −35 °C. Measures of the oxidation potentials can be obtained from the correlation of the irreversible anodic peak potentials E_p.[41] An alternative method for evaluating the potentials used in this study obtains from the intercepts in Figure 3 (left) which according to the Marcus eq 13 is equal to $\sqrt{\lambda}/2 + (\mathcal{F}/2\sqrt{\lambda})(E°_{RM} + w_p/\mathcal{F})$. Judging from the constancy of the slopes, we evaluate λ as 41 kcal mol^{-1} for all alkylmetals. The values of the oxidation potentials (including the work term) are listed as ($E°_{RM} + w_p/\mathcal{F}$) in Table VIII.

Cyclic Voltammetry of TCNE. The standard reduction potential of tetracyanoethylene measured by cyclic voltammetry on a Princeton Applied Research Model 173 potentiostat/galvanostat equipped with a Houston Instrument Series 2000 omnigraphic X-Y recorder. The experiments were carried out in acetonitrile with 0.1 M tetraethylammonium perchlorate as supporting electrolyte, using a platinum working electrode and a saturated NaCl calomel reference electrode. The scan rates were varied between 50 and 600 mV s^{-1}. The separation of 55 mV for the cathodic and anodic peaks corresponded to the theoretical value of close to 59 mV, and the unit ratio of the peak currents i_c/i_a = 1.01 supports a reversible one-electron value. The standard reduction potential of 0.222 V vs. saturated NaCl-SCE corresponds to 0.458 V vs. SHE. The reduction potentials of FeL_3^{3+} and $IrCl_6^{2-}$ were reported earlier.[12]

The reorganization energy of TCNE/$TCNE^-$ was calculated from the rate of electron transfer of 3 × 10^9 M^{-1} s^{-1} for the self-exchange reaction.[17] At $\Delta G° = 0$, $\Delta G^{\ddagger} = \lambda/4 = 2.08$ kcal mol^{-1}, or λ_{TCNE} = 8.3 kcal mol^{-1}.

Acknowledgment. We wish to thank Dr. Jeremy Burdett for helpful discussions, Dr. R. J. Klingler for assistance with the electrochemical measurements, and the National Science Foundation for financial support. We also express our gratitude to the referees who helped in clarifying the presentation.

References and Notes

(1) (a) Marcus, R. J.; Zwolinski, B. J.; Eyring, H. *J. Phys. Chem.* **1954,** *58*, 432. Marcus, R. A. *J. Chem. Phys.* **1956,** *24*, 966. *J. Chem. Phys.* **1957,** *26*, 867. *Discuss. Faraday Soc.* **1960,** *29*, 21. (b) Sutin, N. In "Inorganic Biochemistry", Eichhorn, G. L., Ed.; Elsevier: Amsterdam, 1973; Vol. 2, p. 611. (c) Reynolds, W. L.; Lumry, R. W. "Mechanisms of Electron Transfer"; Ronald Press: New York, 1966. (d) Wilkins, R. G. "The Study of Kinetics and Mechanism of Reactions of Transition Metal Complexes"; Allyn and Bacon: Boston, 1974. (e) Pennington, D. E. *ACS Monogr.* **1978,** *174*, 477.

(2) Hush, N. S. *Trans. Faraday Soc.* **1961,** *57*, 557. *Prog. Inorg. Chem.* **1967,** *8*, 391.

(3) (a) Mulliken, R. S. *J. Am. Chem. Soc.* **1950,** *72*, 600. (b) Mulliken, R. S.; Person, W. B. "Molecular Complexes, a Lecture and Reprint Volume"; Wiley-Interscience: New York, 1969. (c) Mataga, N.; Kubota, T. "Molecular Interactions and Electronic Spectra"; Marcel Dekker: New York, 1970.

(4) Chiu, Y.-N. *J. Phys. Chem.* **1976,** *80*, 992.

(5) (a) Taft, R. W., Jr. In "Steric Effects in Organic Chemistry", Newman, M. S., Ed.; Wiley: New York, 1956. (b) MacPhee, J. A.; Panaye, A.; Dubois, J.-E. *Tetrahedron Lett.* **1976,** 3293.

(6) Evaluated as $I_D(Me_2Hg)$-$I_D(RHgMe)$ from Fehlner, T. P.; Ulman, J.; Nugent, W. A.; Kochi, J. K. *Inorg. Chem.* **1976,** *15*, 2544.

(7) (a) Dulz, G.; Sutin, N. *Inorg. Chem.* **1963,** *2*, 917. (b) Diebler, H.; Sutin, N. *J. Phys. Chem.* **1964,** *68*, 174. (c) Hicks, K. W.; Sutter, J. R. *Ibid.* **1971,** *75*, 1107. (d) Wilkins, R. G.; Yelin, R. E. *Inorg. Chem.* **1968,** *7*, 2667. (e) Campion, R. J.; Purdie, N.; Sutin, N. *Ibid.* **1964,** *3*, 1091. (f) Gordon, B. M.; Williams, L. L.; Sutin, N. *J. Am. Chem. Soc.* **1961,** *83*, 2061.

(8) (a) Compare Halpern, J.; Legare, R. J.; Lumry, R. *J. Am. Chem. Soc.* **1963,** *85*, 680. (b) Halpern, J.; Pribanic, M. *Ibid.* **1968,** *90*, 5942. (c) Abley, P.; Halpern, J. *Chem. Commun.* **1971,** 1238. (d) Sykes, A.; Thorneley, R. F. *J. Chem. Soc. A* **1970,** 232.

(9) For organic substrates, see: (a) Pelizzetti, E.; Mentasti, E.; Pramauro, E. *Inorg. Chem.* **1978,** *17*, 1181. (b) Pelizzetti, E.; Mentasti E.; Barni, E. *J. Chem. Soc., Perkin Trans. 2* **1976,** 623. (c) Pelizzetti, E.; Mentasti, E.; Pramauro, E. *Ibid.* **1976,** 620. (d) Ng, F. T. T.; Henry, P. M. *J. Am. Chem. Soc.* **1976,** *98*, 3606. (e) Cecil, R.; Littler, J. S. *J. Chem. Soc. B* **1968,** 1420; **1970,** 626, 632.

(10) (a) Colter, A. K.; Dack, M. R. J. In "Molecular Complexes", Foster, R., Ed.; Crane Russak & Co.: New York, 1973; Vol. 1, p 301. Vol. 2, 1974, p 1. (b) Compare also Klinger, R. J.; Mochida, K.; Kochi, J. K. *J. Am. Chem. Soc.* **1979,** *101*, 6626.

(11) In common usage, oxidant refers to an inorganic reagent whereas electron acceptor applies to an organic molecule.

(12) Wong, C. L.; Kochi, J. K. *J. Am. Chem. Soc.* **1979,** *101*, 5593.

(13) Gardner, H. C.; Kochi, J. K. *J. Am. Chem. Soc.* **1975,** *97*, 1855.

(14) Chen, J. Y.; Gardner, H. C.; Kochi, J. K. *J. Am. Chem. Soc.* **1976,** *98*, 6150.

(15) Compare also Chen, J. Y.; Kochi, J. K. *J. Am. Chem. Soc.* **1977,** *99*, 1450.

(16) Gardner, H. C.; Kochi, J. K. *J. Am. Chem. Soc.* **1976,** *98*, 2460.

(17) Fukuzumi, S.; Mochida, K.; Kochi, J. K. *J. Am. Chem. Soc.* **1979,** *101*, 5961.

(18) (a) Mulliken, R. S. *J. Am. Chem. Soc.* **1952,** *74*, 811. (b) Orgel, L. E.; Mulliken, R. S. *Ibid.* **1957,** *79*, 4839. (c) Foster, R. "Organic Charge Transfer Complexes"; Academic Press: New York, 1969.

(19) Fukuzumi, S.; Kochi, J. K. *J. Phys. Chem.*, **1980,** *84*, 608.

(20) Clinton, N. A.; Gardner, H. C.; Kochi, J. K. *J. Organomet. Chem.* **1973,** *56*, 227. Clinton, N. A.; Kochi, J. K. *Ibid.* **1973,** *56*, 243.

(21) The activation entropies for FeL_3^{3+}, $IrCl_6^{2-}$, and TCNE range between −20 and −40 eu. [The rather large reorganization energy in eq 14 (vide infra) is mostly associated with the transformation of RM to $RM^{+\cdot}$ since that due to the iron couple is small (see ref 1c, p 44).] The large negative $\Delta S^{\ddagger}$ may be attributed to significant changes in solvation resulting from the sizable values of λ_{RM}.

(22) That is, the correlation between log k and I_D (or its equivalent linear free energy relationship) is directly related to the correlation of $\Delta H^{\ddagger}$ and I_D by the Gibbs–Helmholtz equation. Indeed the slope of 4.9 in Figure 1 is equivalent to the slope of 5.4 in Figure 2, when converted to the same units.

(23) For the evaluation of $E°_{RM}$, see the Experimental Section. $E°_{Fe}$ is tabulated in ref 12.

(24) (a) The same reorganization energy can be obtained from other formulations of the free-energy changes associated with electron transfer. Thus the relationship

$$\Delta G^{\ddagger} = \frac{\Delta G}{2} + \left\{\left(\frac{\Delta G}{2}\right)^2 + \left(\frac{\lambda}{4}\right)^2\right\}^{1/2} \qquad \text{(i)}$$

has been developed [Rehm, D.; Weller, A. *Ber. Bunsenges. Phys. Chem.* **1969,** *73*, 834. *Isr. J. Chem.* **1970,** *8*, 259] empirically. Alternatively, the Levine formulation [*J. Phys. Chem.* **1979,** *83*, 159]

$$\Delta G^{\ddagger} = \Delta G + \frac{\lambda}{4 \ln 2} \ln\left\{1 + \exp\left[-\frac{4\Delta G \ln 2}{\lambda}\right]\right\} \qquad \text{(ii)}$$

is equivalent to the Marcus equation[36]

$$\Delta G^{\ddagger} = \frac{\lambda}{4} + \frac{\Delta G}{2}[1 + \ln \cosh y/y] \qquad \text{(iii)}$$

where $y = 2\Delta G \ln 2/\lambda$. (b) For example, for Et_4Sn with $\Delta G^{\ddagger}$ = 14.1 kcal mol^{-1} and ΔG = 7.0 kcal mol^{-1}, λ is calculated as 40 and 41 kcal mol^{-1} using eq i and ii, respectively. (In eq ii, λ is determined numerically.) (c) The relationship among the free-energy formulations in eq i, ii, and iii has been recently discussed [Scandola, F.; Balzani, V. *J. Am. Chem. Soc.*

1979, *101,* 6142].

(25) The reversible reduction potentials of TCNE and $IrCl_6^{2-}$ in acetonitrile are 0.46 and 0.67 V vs. SHE, respectively.[10b,12] For TCNE, $\Delta G = \mathcal{F}(E^\circ_{RM} - 0.46) + w_p$; for $IrCl_6^{2-}$, $\Delta G = \mathcal{F}(E^\circ_{RM} - 0.67) + w_p$ where $E^\circ_{RM} + w_p/\mathcal{F}$ is obtained from Table VIII. The work term is assumed to be the same.

(26) The reorganization energy $\lambda = (\lambda_{11} + \lambda_{22})/2$, where λ_{11} is related to the self-exchange reaction of $RM/RM^{+\cdot}$ and λ_{22} to that of $FeL_3^{3+,2+}$, TCNE/$TCNE^{-\cdot}$, or $IrCl_6^{2-,3-}$.[1] When λ_{22} for FeL_3^{3+} is taken as zero,[1c] the corrected reorganization energy is $\lambda = 41 + \lambda_{22}/2$. The solid line for $\Delta G^\ddagger$ is recalculated from eq 12 using λ_{22}(TCNE) and $\lambda_{22}(IrCl_6^{2-})$ of 8.3 and 26 kcal mol^{-1}, respectively.

(27) Equation 12, originally derived for the region of weak overlap, has been applied to reactions with considerable resonance splitting such as inner-sphere electron transfers, proton transfers, and atom transfers in which the meanings of the terms are modified.[28]

(28) (a) Sutin, N. *Annu. Rev. Phys. Chem.* **1966,** *17,* 154. (b) Haim, A.; Sutin, N. *J. Am. Chem. Soc.* **1966,** *88,* 434. (c) Patel, R. C.; Endicott, J. F. *Ibid.* **1968,** *90,* 6364. (d) Linck, R. G. *MTP Int. Rev. Sci.: Inorg. Chem., Ser. One* **1971,** *9,* 303. (e) Fan, F. F.; Gould, E. S. *Inorg. Chem.* **1974,** *13,* 2647. (f) Linck, R. G. *Surv. Prog. Chem.* **1976,** *7,* 89. (g) Durham, B.; Endicott, J. F.; Wong, C. L.; Rillema, D. P. *J. Am. Chem. Soc.* **1979,** *101,* 847. (h) Kresge, A. J. In "Proton Transfer Reactions", Caldin, E., Gold, V., Eds.; Chapman and Hall: London, 1975; p 179 ff.

(29) (a) The importance of the work term has been noted in outer-sphere cross reactions with ions of opposite charges [Haim, A.; Sutin, N. *Inorg. Chem.* **1976,** *15,* 476]. (b) Steric effects may also affect the reorganization energies but are not included in this qualitative discussion (however, see Figure 9).

(30) Foster, R. In ref 10a, Vol. 2, p 107.

(31) Tamres, M.; Strong, R. L. In "Molecular Association", Foster, R., Ed.; Academic Press: New York, 1979; Vol. 2.

(32) Importantly, the comparative definition of ΔE in eq 17 minimizes solvation terms by cancellation. Thus it can be used directly for the work term in the free-energy change for inner-sphere electron transfer. (In contrast, the *absolute* value of the interaction energy ω in the vertically excited CT state differs from the work term w_p in thermal ion pairs since the latter includes a significant contribution from solvation, whereas ω does not.)

(33) Excluding vibronic states, the principal difference between these ion pairs lies in the mean separation parameters, $r^\ddagger$ and r_{DA}, for the thermal and photochemical processes, respectively. [For potential-energy diagrams illustrating the relationship between the thermal ($r^\ddagger$) and photochemical (r_{DA}) processes in CT interactions, see ref 17.] Thus, it is implicit in this treatment that as a result of steric effects the *relative change* of the mean separation in the CT excited state is the same as that in the thermal ion pair.

(34) The Brønsted slope $\alpha = 1$ corresponds to a slope of 9.4 in the plot of log k vs. I_D, since $I_D = 1.8\Delta G +$ constant (ref 12).

(35) It is remarkable that ΔE obtained for TCNE can be applied to $IrCl_6^{2-}$. The selectivities in Table III suggest that the ion pairs are similar, which may account for its success.

(36) Marcus, R. A. *J. Phys. Chem.* **1968,** *72,* 891.

(37) Since the microscopic reverse represents a diffusion-controlled electron transfer, In qualitative terms eq 20 and 22 can be related to the Hammond postulate for endothermic processes.

(38) In order to present the inner-sphere slope (*b*) for TCNE and $IrCl_6^{2-}$ in Figure 9, C in eq 20 was taken as -11.6 kcal mol^{-1}, which is the difference between $\Delta G^\ddagger = 21.6$ kcal mol^{-1} and $\Delta G = 33.2$ kcal mol^{-1} for Me_4Sn and TCNE, respectively, since $\Delta G^\ddagger$ cannot be smaller than ΔG. For Me_4Sn and $IrCl_8^{2-}$, the difference is 7.6 kcal mol^{-1} (i.e., $\Delta G^\ddagger - \Delta G = 20.8 - 28.4$). In computing curve (*b*), λ was taken as 20 kcal mol^{-1}. After the Brønsted slope of eq 12 exceeded unity, eq 22 was used. (See comments by Scandola and Balzani.[24c]) Compare also Efrima, S.; Bixon, M. *Chem. Phys.* **1976,** *13,* 447.

(39) Since the outer-sphere work term for FeL_3^{3+} in eq 20 is taken to be nil,[1c] ΔG in Figure 3 is relabeled as ΔG° here.

(40) The value of Δw_p chosen is a minimum value corresponding roughly to C in eq 20.[38] The actual difference between the outer-sphere and inner-sphere correlations in Figure 9 will be larger, i.e., the latter will be shifted to the right. Although it can be larger, the actual value of Δw_p will not affect the general discussion in Figure 9 relating to the shift from the outer-sphere correlation to the inner-sphere correlations in curves (*a*) and (*b*) by changing the magnitudes of w_p and λ_{RM}.

(41) Klingler, R. J.; Kochi, J. K. *J. Am. Chem. Soc.*, accepted for publication.

Isomers of *closo*-Dicarbapentaborane(5) and Their Methyl and Fluoro Derivatives. A Theoretical Study

Glenn D. Graham,[1a] Dennis S. Marynick,[1b] and William N. Lipscomb*[1a]

Contribution from the Gibbs Chemical Laboratory, Harvard University,
Cambridge, Massachusetts 02138, and the Department of Chemistry,
The University of Texas, Arlington, Texas 76019. *Received August 8, 1979*

Abstract: Relative energies have been calculated using the partial retention of diatomic differential overlap (PRDDO), STO-3G, and 4-31G methods for $(CH)_2(BH)_3$, $(CH)_2(BH)_2BCH_3$, and $(CH)_2(BF)_3$ in the isomeric 1,5-trigonal bipyramidal (I), 1,2-planar (II), 1,2-trigonal bipyramidal (III), 2,3-square planar (IV), 1,3-planar (V), and 2,3-trigonal bipyramidal (VI) geometries, optimized at the PRDDO level. The 1,5-TBP form is considerably more stable than the other structures for $C_2B_3H_5$ and for $(CH)_2(BH)_2BCH_3$, although the 1,2-planar isomer is almost as stable as the 1,5-TBP for $(CH)_2(BF)_3$. The planar, "classical" forms are comparable in energies to the 1,2-TBP and the other nonclassical isomers of $C_2B_3H_5$ and $(CH)_2(BH)_2BCH_3$. Localized molecular orbitals are examined, and some isomerization pathways are discussed among these isomers.

The term "superaromatic" has been used[2a] to characterize the relative unreactivity, stability, and symmetrical bonding patterns in the *closo*-carboranes $C_2B_{n-2}H_n$ and their isoelectronic dianions $B_nH_n^{2-}$. These polyhedral species undergo isomerizations which are still under active study.[2b,3] For $n = 5$ only the 1,5-trigonal bipyramidal $C_2B_3H_5$ has been isolated,[4] although C,3-$(CH_3)_2$-1,2-$C_2B_3H_3$, 3,4,5-$(CH_3)_3$-1,2-$C_2B_3H_2$, C,3,4,5-$(CH_3)_4$-1,2-C_2B_3H, and C′,3,4,5-$(CH_3)_4$-1,2-C_2B_3H have also been obtained.[5] One question which we study here is whether there is some special thermodynamic stability or lack of reactivity associated with methylation. These observations and questions will lead us to reexamine the nonclassical three center bond structures relative to the classical structures having formally trigonal boron atoms in the smallest known, probably most anomalous member of the *closo*-carboranes. Furthermore, we shall find that methyl substitution for H does not confer unusual stability, but that fluorine substitution does drastically favor "classical" structures. The question of energy wells high above the most stable isomer of $C_2B_3H_5$ will arise for trigonal-bipyramidal 1,2-$C_2B_3H_5$. Finally, numerous plausible (but not all possible) isomerization pathways will be examined.

Some limited theoretical aspects of the complex structural chemistry of this system have been discussed previously.[6-10] Our preliminary results[11] have introduced the concept of the classical to nonclassical to classical conversion in isomerization of carboranes and boron hydride anions, and have indicated circumstances in which halogen substitution might favor "classical" structures. Examples of the halogen effect previously known are B_2H_6 vs. BF_3 or B_2F_4, of *nido*-$C_4B_2H_6$[12] vs. planar $(CH)_4(BF)_2$,[13] of $B_8H_8^{2-}$ vs. B_8Cl_8, and of nonexistent B_4H_4 vs. known B_4Cl_4.

0002-7863/80/1502-2939$01.00/0